MAGNETIC FIELD MEASUREMENTS OF HD2, A HIGH Nb_3Sn DIPOLE MAGNET

X. Wang, S. Caspi, D. W. Cheng, H. Felice, P. Ferracin, R. R. Hafalia, J. M. Joseph, A. F. Lietzke, J. Lizarazo, A. D. McInturff, G. L. Sabbi

Lawrence Berkeley National Laboratory, 1 Cyclotron Road, Berkeley CA 94720

K. Sasaki

KEK, Tsukuba, Ibaraki 305-0901, Japan

DISCLAIMER

This document was prepared as an account of work sponsored by the United States Government. While this document is believed to contain correct information, neither the United States Government nor any agency thereof, nor The Regents of the University of California, nor any of their employees, makes any warranty, express or implied, or assumes any legal responsibility for the accuracy, completeness, or usefulness of any information, apparatus, product, or process disclosed, or represents that its use would not infringe privately owned rights. Reference herein to any specific commercial product, process, or service by its trade name, trademark, manufacturer, or otherwise, does not necessarily constitute or imply its endorsement, recommendation, or favoring by the United States Government or any agency thereof, or The Regents of the University of California. The views and opinions of authors expressed herein do not necessarily state or reflect those of the United States Government or any agency thereof or The Regents of the University of California.

This work was supported by the Director, Office of Science, Office of Fusion Energy Sciences, of the U.S. Department of Energy under Contract No. DE-AC02-05CH11231.

MAGNETIC FIELD MEASUREMENTS OF HD2, A HIGH FIELD Nb_3Sn DIPOLE MAGNET*

X. Wang†, S. Caspi, D. W. Cheng, H. Felice, P. Ferracin, R. R. Hafalia, J. M. Joseph, A. F. Lietzke, J. Lizarazo, A. D. McInturff, G. L. Sabbi, LBNL, Berkeley, CA 94720, USA
K. Sasaki, KEK, Tsukuba, Ibaraki 305-0801, Japan

Abstract

The Superconducting Magnet Program at Lawrence Berkeley National Laboratory has designed and tested HD2, a 1 m long Nb_3Sn accelerator-type dipole based on a simple block-type coil geometry with flared ends. HD2 represents a step toward the development of cost-effective accelerator quality magnets operating in the range of 13–15 T. The design was optimized to minimize geometric harmonics and to address iron saturation and conductor magnetization effects. Field quality was measured during recent cold tests. The measured harmonics are presented and compared to the design values.

INTRODUCTION

The HD dipole magnet series features a simple block-type coil design. After the successful test of HD1, reaching a record magnetic field of 16 T [1], HD2 was designed and tested, representing a step toward the development of cost-effective accelerator-type magnets operating in the range of 13–15 T [2, 3, 4].

HD2 is 1 m long with flared ends. The bore clearance is 36 mm with a stainless bore tube and increases to 43 mm when the tube is removed. At 4.3 K, the short sample current (I_{ss}) of HD2 is 18.1 kA, corresponding to a bore field of 15.6 T and a coil peak field of 16.5 T [5]. Four tests have been completed for HD2 and a bore field of 13.8 T (87% I_{ss} based on virgin strand I_c measurement) was reached. More details about the magnet parameters and the first three tests are found in [5]. In the fourth test (HD2d), the first magnetic field measurements using a rotating coil were taken.

In this report, the experimental details are presented first, followed by the measured and computed results. The coil end optimization for minimizing b_3 is discussed.

EXPERIMENTAL SYSTEM AND PROCEDURES

The magnet was positioned vertically in the test cryostat. Inside the magnet bore was an anti-cryostat housing the rotating coil. The heater embedded in the anti-cryostat provided a room-temperature environment to ensure the proper rotation of the coil. The rotating coil has a radius of 11.66 mm and a length of 100.01 cm, slightly longer than the magnet coil (including end regions). The coil has seven windings, including one tangential coil, two bucked dipole coils, and four bucked quadrupole coils. The probe rotated at a speed of $\sim$ 0.5 Hz. In every revolution, a chain of 4096 pulses (phase A) and one pulse (phase Z) were generated by an incremental encoder mounted at the end of the probe. The probe movement along the axial (z) direction, parallel to the magnet bore, was controlled by a step motor with a resolution of $\sim 2\ \mu$m.

Tangential and bucked dipole voltages were amplified by a front-end amplifier assembly before being digitized. A high-resolution dynamic signal acquisition card (NI4472B, 24-bit) was used to digitize the inputs simultaneously. The sampling had to be driven by the NI4472B internal clock and as a result, the encoder signals were also recorded by the NI4472B to calculate the flux at specific angular positions. The sampling frequency (f_s) was 102.4 kHz, the highest allowed by the NI4472B. It was about four orders of magnitude higher than that of the 20th field harmonic. The magnet current was digitized by an NI6221 card (16-bit) with a resolution of 0.6 A. The period of phase A pulses (Δt) was also measured by the NI6221. The PXI-based data acquisition system was controlled by a LabWindows/CVI program.

The flux $\psi(k)$ at an angular position θ_k is given by $\psi_k = \psi_{k-1} + \Delta\psi_{k-1}$, where $k = 1, \ldots, 4095$ and $\psi_0 = 0$ [6]. The flux increment between the $(k-1)$th and the kth phase A pulses is estimated by $\Delta\psi_{k-1} = -\sum_{i=0}^{N-1} V(t_i)\delta t/G$, where $\delta t = 0.1/f_s$ and $N\,\delta t = \Delta t$. $V(t_i)$ is the voltage at t_i linearly interpolated between two measured data points. G is the amplifier gain for V. The flux data was then reduced into multipole coefficients through a discrete Fourier transform. The rising/falling edges of phase A/Z signals were recognized by the data analysis program. The difference between the Δt calculated by the program and those measured by the NI6221 is typically within 10 μs, $\sim 2\%\Delta t$.

RESULTS AND DISCUSSION

Two sets of measurements were taken: 1) ramp measurement during the current up-ramp with fixed z position of the probe and 2) DC measurements at 10 kA at various z positions. Here z is the position of the rotating coil center with respect to the magnet center. Given $BL_{\mathrm{eff},z=0}$ the

* This work was supported by the Director, Office of Science, Office of Basic Energy Sciences, of the U. S. Department of Energy under Contract No. DE-AC02-05CH11231.

† xrwang@lbl.gov

integrated dipole strength in T-m when the centers of the rotating coil and the magnet aligned, the multipole coefficients b_n in 10^{-4} unit at $R_{\rm ref} = 11.66$ mm was estimated by

$$b_n = \frac{10^4 B_{n,z}}{2R_c T \frac{K_n}{n} \left(\frac{R_c}{R_{\rm ref}}\right)^{n-1} BL_{{\rm eff},z=0}}, \qquad (1)$$

where $B_{n,z}$ is the real Fourier coefficient of the nth order as a function of the probe position; R_c is the coil radius in m; T the number of turns in the tangential coil; K_n is the normalized bucked sensitivity for the nth harmonic ($n = 1$ for dipole).

Ramp Measurements

Measurements were taken when the magnet current ramped up from 0 to different levels with a highest of 15.2 kA (84% I_{ss}). The ramp rate decreased from 75 A/s to 50 A/s at 5 kA and reduced to 20 A/s at 9 kA. The probe center was 3 cm below the magnet center. In the 15.2 kA measurement, however, data were noisy above 8.5 kA and the reason is not clear yet. Thus, a measurement with a peak current of 10.6 kA was shown in Fig. 1, where the computed geometric and the measured b_3 integrated over a length of 1 m as a function of current were compared.

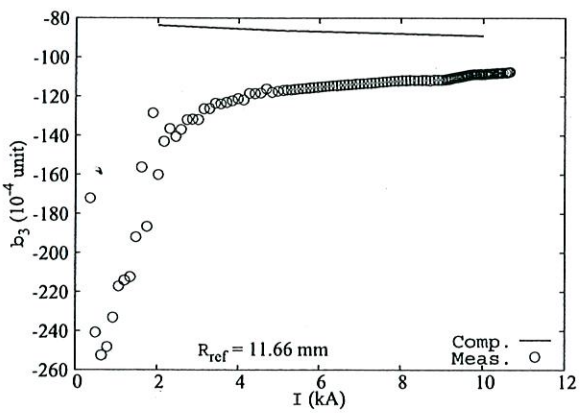

Figure 1: Normalized sextupole (b_3, integrated over a length of 1 m) as a function of magnet current (up-ramp).

The discrepancy seen from 0 to 10 kA may result from that the measurement was only taken during the current up-ramp. At low current, the high b_3 was dominated by the persistent current, which can be corrected as a next step [4]. At high current, it was dominated by the effect of the coil ends, which will be discussed in the last section.

DC Measurements

The DC measurements were performed at 10 kA. At least four measurements were taken for each z position and the averaged values were reported. The probe was rotating in one direction for all cases.

Figure 2 compares the axial dependence of the sextupole integrated over a length of 1 m and normalized relative to the magnet center. Within ± 0.2 m of the magnet center, the amplitude of the measured b_3 increased and peaked (-100.0 units) at the magnet center, while outside of this range the measured b_3 was constant at -50.0 units. At -3 cm, both the measured and computed values were consistent with the peak values shown in Fig. 1. The high b_3 values resulted from the magnet ends, both covered by the 1 m long rotating coil.

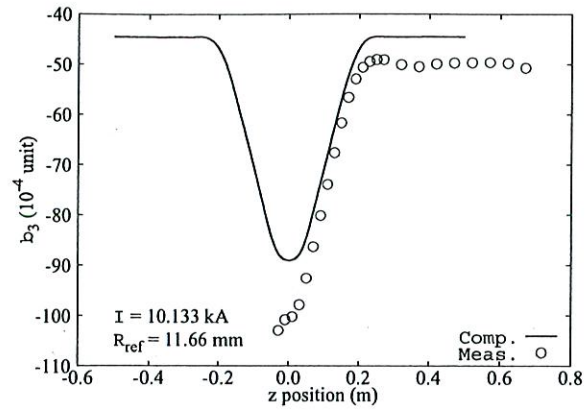

Figure 2: Axial dependence of the sextupole (b_3, integrated over a length of 1 m) relative to the magnet center.

Figure 3 shows the axial dependence of the decapole (b_5) integrated over a length of 1 m and normalized relative to the magnet center. The measured b_5 ranged from -5.0 units to -5.3 units within ± 0.1 m of the magnet center. It then reduced quickly to -3.0 units at ± 0.2 m with respect to the magnet center.

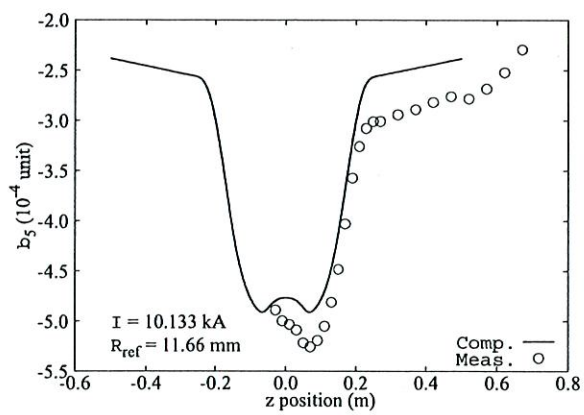

Figure 3: Axial dependence of the decapole (b_5, integrated over a length of 1 m) relative to the magnet center.

At the magnet center, $b_{7,\,\rm meas.} = -0.2$ units and $b_{7,\,\rm calc.} = -0.6$ units. From Figs. 2 and 3, one sees that the measured results followed the same profile of the computed values, even though consistently higher than the computed values. The reasons for the discrepancy may include: 1) the effect of the persistent current as seen in the AC measurement, 2) the ideal situations used by the simulation. For example,

the model considered only the return end of the coil, while the lead end features one turn less because of the ramp configuration. Since the length of the rotating coil was slightly longer than the magnet coil, the effect of the current leads may also contribute to the measurement error. As a next step, these effects will be analyzed in more detail.

Coil End Optimization

The presence of flared ends represents one of the main features of the HD2 coil design. At the end of the straight section, approximately 480 mm long, a gentle hard-way bend is introduced to transition the blocks into a 10° flare (see Fig. 4). After the hard-way bend of the cables, a flat racetrack end configuration is recovered (except for the transition turn), on a plane inclined by 10° with respect to the magnet axis.

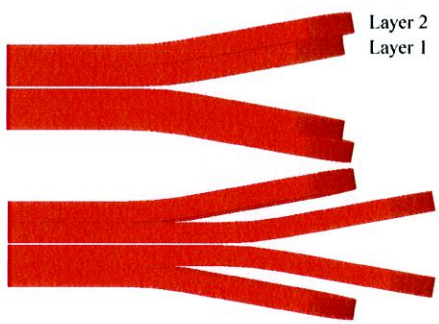

Figure 4: Coil design of HD2 (top) and configuration optimized to reduce integrated harmonics in the ends (bottom).

The magnetic measurements shown in the previous sections, and confirmed by numerical computations, indicated that the b_3 integrated over a length of 1 m reached 50 units ($R_{\mathrm{ref}} = 11.66$ mm) in the end region. The origin of this level of b_3 can be attributed to the particular design of the HD2 coil ends. In fact, if a finer estimate of the variation of the sextupole along the magnet axis is performed by integrating over a shorter length (8 mm instead of 1 m), one can notice that the b_3 features two spikes in correspondence of the tilted ends (0 mm offset curve in Fig. 5).

A possible corrective strategy to reduce the harmonics in the end region consists in shifting axially the first layer with respect to the second layer (see Fig. 4 bottom). Figure 5 shows how the integrated b_3 can be progressively reduced by a relative axial shift between the two layers. This modification will be considered in future optimized designs.

CONCLUSION

Magnetic field of HD2, a high-field Nb_3Sn dipole, was measured. The rotating coil is 100.01 cm long, similar to the length of the magnet. The high b_3, as shown by both the computed and measured results, can be attributed to the particular design of the HD2 coil ends. A possible corrective strategy to reduce the harmonics in the end region

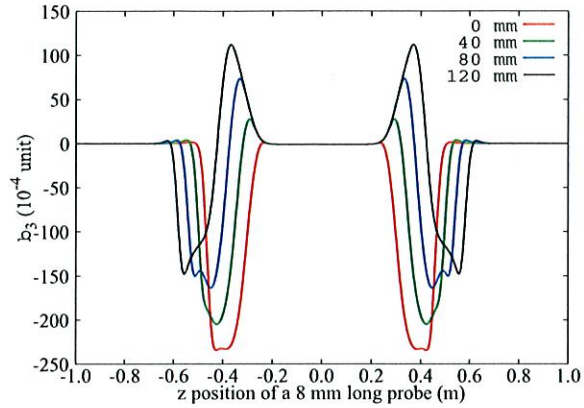

Figure 5: Computed variation along the magnet axis of the b_3 integrated over a length of 8 mm. The curves are associated to different coil designs, where the first layer has been shifted axially with respect to the second layer.

consists in shifting axially the first layer with respect to the second layer.

The measured geometric harmonics integrated over a length of 1 m were generally in good agreement with the computed values. Persistent current effect dominated the high b_3 at low current, which could be corrected based on detailed measurements on the persistent current effect.

A second measurement to use shorter probes and to measure at high currents is under preparation. It will allow a comparison between the measurements using different probes, in addition to a finer estimation of the field quality in HD2 for further optimization.

ACKNOWLEDGMENTS

We thank the technical staff of the program for their support.

REFERENCES

[1] A. F. Lietzke *et al.*, "Test results for HD1, a 16 Tesla Nb_3Sn dipole magnet," *IEEE Trans. Appl. Supercond.*, vol. 14, no. 2, pp. 345–348, 2004.

[2] G. Sabbi *et al.*, "Design of HD2: a 15 Tesla Nb_3Sn dipole with a 35 mm bore," *IEEE Trans. Appl. Supercond.*, vol. 15, no. 2, pp. 1128–1131, June 2005.

[3] P. Ferracin *et al.*, "Mechanical design of HD2, a 15 T Nb_3Sn dipole magnet with a 35 mm bore," *IEEE Trans. Appl. Supercond.*, vol. 16, no. 2, pp. 378–381, June 2006.

[4] P. Ferracin *et al.*, "Development of the 15 T Nb_3Sn dipole HD2," *IEEE Trans. Appl. Supercond.*, vol. 18, no. 2, pp. 277–280, 2008.

[5] P. Ferracin *et al.*, "Assembly and test of HD2, a 36 mm bore high field Nb_3Sn dipole magnet," *IEEE Trans. Appl. Supercond.*, vol. 19, no. 3, 2009, in press.

[6] L. Bottura, "Standard analysis procedures for field quality measurement of the LHC magnets — part I: harmonics," LHC/MTA, Tech. Rep. LHC-MTA-IN-97-007, 2001.